LAWRENCE
LIVERMORE
NATIONAL
LABORATORY

LLNL-TR-795754

Amorphous carbon coatings with controlled density and composition

S. Falabella, J. S. Miller, A. Ceballos-Sanchez, S. O. Kucheyev, S. Elhadj

October 31, 2019

Disclaimer

This work performed under the auspices of the U.S. Department of Energy by Lawrence Livermore National Laboratory under Contract DE-AC52-07NA27344.

FINAL REPORT

Amorphous Carbon Coatings with Controlled Density and Composition

Steven Falabella (19-FS-013)

IM release #LLNL-JRNL-XXXXXX

Abstract

Inertial confinement fusion (ICF) experiments rely on the compression of a spherical capsule containing tritium and deuterium fuel as a way to achieve thermonuclear fusion. Rapid ablation of the capsule surface produces the reactive force that compresses the capsule. Carbon-based capsule materials currently used include low-density glow discharge polymer (GDP) and polycrystalline diamond. An ideal capsule material would have the high density of diamond, with the amorphous nature of GDP, which would reduce asymmetries during compression caused by a random crystalline structure. An intermediate material, diamond-like carbon (DLC), has an amorphous structure, and densities between GDP and diamond, but has been difficult to produce with low stress and low impurity levels. The goal of this Feasibility Study was to investigate the practicality of using a magnetically enhanced, hollow-cathode, plasma source to produce thick (50-200 μm), low-stress, diamond-like carbon films for ICF ablator applications.

The coatings produced during the course of this work have been shown to be amorphous, to have a higher density than traditional GDP ablators (1.6-1.7 g/cc), to have low stress (67-113 MPa), and can be deposited at the high thicknesses required for ICF capsule requirements. Atomic-force microscopy on a 45-micron-thick coating also measured the films to have grain sizes on the order of 20 nanometers, and a root-mean-squared surface roughness of 0.5 nanometers.

Background and Research Objectives

Inertial Confinement Fusion (ICF) experiments at the National Ignition Facility (NIF) are attempting to generate fusion via indirect drive by x-ray heating and compression of a spherical capsule filled with deuterium and tritium fuel. Current indirect drive experiments utilize either low-density GDP, beryllium, or high-density carbon (polycrystalline diamond) ablators for the compression of target capsules. [1,2] GDP based ablators are amorphous, easily accept dopants, and have low surface roughness but have low density (~1.1 g/cc), and are highly affected by support tents [1-4]. Beryllium-based ablators have higher density (1.85 g/cc) but are difficult to work with due to their high toxicity and surface roughness. [1,2,5] Diamond ablators have the highest density (~3.5 g/cc), are mechanically strong, and have high thermal conductivities. Current simulations predict high-density carbon to have the best yields followed by GDP, and not enough information on beryllium is available to make accurate predictions. Diamond ablators suffer from drive instabilities due to its crystalline structure, leading to

asymmetric compression of the capsule during indirect drive. Diamond also has remained a difficult material to produce with custom impurity concentrations [1,2,6]. An ideal ablator would have the high density and mechanical strength of diamond with the amorphous nature of GDP. Therefore, it is highly desired to develop a diamond-like carbon with a density between GDP and diamond, while maintaining an amorphous structure, and is accepting of dopants.

Synthesis of diamond-like carbon has been a topic of interest for decades due to its high hardness, corrosion resistance, high thermal conductivity, and tunable refractive index [7-10]. This material can go by many different names: amorphous carbon (a-C), tetrahedral amorphous carbon (ta-C), hydrogenated amorphous carbon (a-C:H) depending on the hydrogen content, and sp2-to-sp3 bond ratio of the films [11]. DLC films are of high interest to ICF applications because high density and mechanically robust films with amorphous character have been reported [12]. However, most applications for DLC only require film thicknesses ranging from hundreds of nanometers to a few microns. For film thicknesses beyond this range, controlling the film stress becomes critical for utilizing the properties of amorphous carbon [12-14]. Ablators for ICF range between 50 and 200 μm, depending on material density. Therefore, a major goal of this study is to produce low-stress, amorphous carbon films in this thickness range.

There are many reported ways to develop diamond-like carbon films including: filtered cathodic arc, magnetron sputtering, pulsed laser deposition, and plasma-enhanced chemical vapor deposition [15-27]. Filtered cathodic arc appears to have developed the densest amorphous carbon films, reaching densities up to 2.7 g/cc with hydrogen content less than 1%. The drawback of this process being the high stress of films generated along with a large number of particulates contaminating the coatings [12, 15-17]. Other PVD based techniques have been able to demonstrate adequately dense films with good doping characteristics [10, 22].

Chemical vapor deposition processes of diamond-like carbon utilize a hydrocarbon gas source mixed with a diluting gas under a plasma, typically produced by either a 13.56 MHz radio frequency (RF) or 2.45 GHz microwave excitation [24, 27-28]. The hydrocarbon gas disassociates in the plasma and impinges on a substrate, creating a carbon film. In many cases, diluting gases such as nitrogen, argon, and neon are used as ionization aids for the hydrocarbon plasma [25]. Hydrogen can also be utilized, but typically lower density films are formed, similar to glow discharge polymers [29]. By tuning the reactor pressure, gas-feed composition, and plasma characteristics a film with low stress, and high rate, and density can ideally be achieved.

In this study, we fabricated and tested a magnetically enhanced, RF-powered hollow cathode, CVD system for coating diamond-like-carbon with low stress at significant thicknesses. We covered a wide range of operational parameters and noted their effects on film quality, deposition rate, plasma stability, and density.

Scientific Approach and Accomplishments

All coatings were performed in a custom, LLNL-designed RF-driven, hollow cathode system enhanced by a variable magnetic field. A schematic for the system can be seen in Figure 1. Propylene (99.9% purity, Matheson Inc.) was utilized as the hydrocarbon source. Propylene was chosen as a compromise between the lower C/H ratio of methane, and the difficulties working with acetylene. Ultra-high purity

(UHP) Hydrogen (99.9%, Matheson Inc.) was initially utilized as the diluting gas for experiments. Nitrogen and UHP argon were also used as additional diluting gas sources. Coatings were deposited onto 1.9 cm x 1.3 cm silicon wafers attached to a water-cooled sample holder, located approximately 3 inches away from exit aperture of the hollow cathode. Prior to coating, the chamber was pumped down to between 3E-5 and 4E-5 Torr using a turbomolecular pump backed by a small roughing pump. Propylene gases and diluting gases were introduced through the hollow cathode, and impinged onto the substrate surface. An RF power supply was used to ionize the gas mix inside the hollow cathode with powers between 25 and 150 watts (W). A magnetic field was produced by a direct-current (DC) carrying coil placed around the tube of the vacuum chamber containing the hollow cathode This field enhanced the discharge and stabilized the plasma at lower operating pressures. Percentage of propylene in the propylene/ diluting gas feed ranged between 5% and 100% propylene, with operating pressures between 3 and 40 milliTorr.

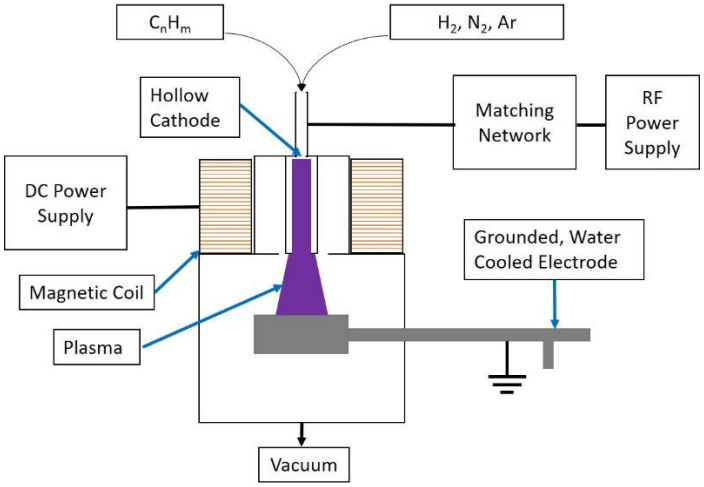

Figure 1. Schematic for Magnetically Confined RF Plasma Hollow cathode for Coating Diamond-Like-Carbon

Film thicknesses were measured via stylus profilometry (KLA Tencor, Inc.) at the edge of a masked section on one end of the silicon substrate, and were used along with deposition times to calculate rates. Densities were measured on a mass micro-balance before and after coating while the coating volume was taken as the thickness of the film times the area of the wafer (minus the area of the masked region). Stylus profilometry was also used to estimate the stress on films by measuring the radius of curvature of the coated silicon sample, and applying the Stoney Equation [30].

Optical emission spectroscopy (OES) was used to monitor the plasma conditions during varying operational conditions, utilizing a Thorlabs CCS200-Compact Spectrometer with a range between 200 and 1000 nm. A 4-inch extension tube with a window was added to the side port of the vacuum chamber to reduce coating on the window, and the fiber optic input to the spectrometer was pointed directly at the plasma.

Raman spectroscopy was used to characterize the molecular bonds in the coatings using an excitation wavelength of 632.8 nm from a He-Ne laser. Compositional characterization was done using Rutherford Backscattering Spectrometry (RBS) with 2

MeV $^4He^+$ ions incident parallel to the normal of the sample and backscattered into a detector at 164 degrees. The analysis of the RBS spectra was done using SIMNRA [34]. Hydrogen content was measured using elastic recoil detection analysis (ERDA) with 3 MeV $^4He^+$ ions.

Initially, a wide parameter space was explored as demonstrated in Table 1. Early attempts using propylene-only plasmas yielded high deposition rates, but immediate flaking of the coating during deposition. Propylene concentrations over 40% typically yielded higher deposition rates, accompanied by coating flaking and extremely low plasma stability at lower operating pressures. Samples with propylene feed content below 40% typically performed best in terms of plasma stability and film stress, with 20-30% propylene feed being an optimal balance between deposition rate, film density, and plasma stability.

The diluting gas chemistry also plays a huge role in the quality of the films deposited. Utilizing hydrogen as the diluting gas typically lead to higher deposition rates (up to 6 µm/hr). However, the minimum pressure for stable plasma with the hydrogen plasma was greater than 10 mTorr. The films produced with a hydrogen plasma were low density, contained high concentrations of oxygen, and experienced high compressive stress over time leading to delamination.

Table 1. Overview of Coating Runs and Conditions

Conditions	Film Quality/Stresses	Plasma Pressure Stability	Deposition Rates	Density	Impurity Content
Propylene Content > 40%	High (depositing particulates at high rates vs films)	>10 mTorr	High (Up to 10 µm/hr)	No Data	Dependent on Diluting Gas
Propylene Content <40%	Dependent on Diluting Gas	Dependent on Diluting gas (3-10 mTorr)	Medium (Up to 6 µm/hr)	Dependent on Diluting Gas	Dependent on Diluting Gas
H_2 Diluting Gas	High Compressive Stress over time	10 mTorr	High (6 µm/hr)	Low (1-1.3 g/cc)	Medium (O contaminants)
N_2 Diluting Gas	Low Stress	3 mTorr	Low (0.78 µm/hr)	High (1.5-1.6 g/cc)	Med (1-4 at% Fe, 10% at N, 1-5% Oxygen)
N_2 Gas Flow Through Outside Hollow Cathode	No Data	7.5 mTorr	Low (0.6 µm/hr)	Low (1.4 g/cc)	High (O, N, and Fe contaminants)
Ar Diluting Gas	Low Stress	2.5 mTorr	Low (0.25 µm/hr)	High (1.7 g/cc)	Low (1-4 at% Fe)
High Power (>75 W)	Poor Coating Quality→ No Deposition	3 mTorr	No Deposition	No Deposition	No Data

Switching the diluting gas to either N_2 or Ar led to a significant drop in rate (0.78 µm/hr for N_2 and 0.25 µm/hr for Ar) but yield higher density films (1.6 g/cc for N_2 and 1.7 g/cc for Ar). Operating with either dilutant caused slight sputtering of the stainless-steel hollow cathode surface, contaminating films with up to 4 atomic percent iron. Nitrogen usage lead to nitrogen incorporation into films. Most experiments in this study were performed using a nitrogen diluting gas for its low stress, and higher rate. Overall, the most successful samples were done at 3 milliTorr with a 20-30% propylene blend balanced with either argon or nitrogen, and 10 A current applied to the magnetic field coil. Changing the power and the magnetic field have significant results on the process and therefore the quality of the coating.

Figure 2A shows how the RF power affects the deposition rate and the self-bias voltage hollow cathode. After 75 W, it is currently believed that the nitrogen ions are receiving sufficient energy to kinetically sputter etch the coating as its deposited. The cross over between coating and etching for this experiment occurs at a bias voltage of -150 V. The etching process could also be attributed to hydrogen chemical etching after the hydrogen is cracked from the propylene plasma, leading to the output formation of silane. Future experiments may include using lighter diluting gases to examine the effects of sputter versus chemical etching.

The applied magnetic field also influences the self-bias voltage on the hollow cathode as demonstrate in Fig. 2B. An interesting phenomenon is seen, that at a certain magnetic field strength (~9 A in the coil) the bias voltage reaches a local minimum, independent of the power supplied. Other researchers have also noticed this effect [31-33].

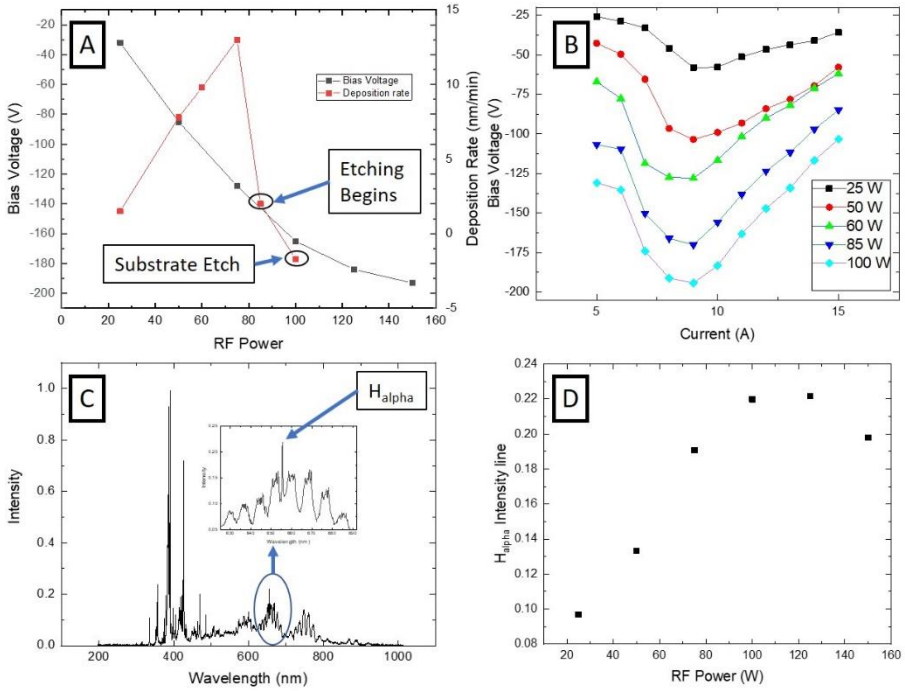

Figure 2. The effects of plasma conditions (power and magnetic coil current) on the (A) deposition rate, (A&B) Bias Voltage, (C) the optical emission spectra, and (D) the H_{alpha} intensity

Optical emission spectroscopy was utilized to analyze the plasma generated during the ionization process. Figure 2C. shows a reference spectrum of an ~ 20/80 propylene mixture at 3 milliTorr, 10 A of current and 100 W of RF power. This spectrum is nearly 100% identical to that of a nitrogen spectrum. Most of the propylene emission lines lie within the same wavelength regime as nitrogen, making them difficult to resolve. Two peaks, however, were resolved, corresponding to the H_{alpha} (656 nm) and the H_{beta} (485 nm) emission peaks. Since no additional hydrogen is being supplied to the chamber it is believed the hydrogen peaks are associated with hydrogen disassociated from the propylene precursor gas. Because of the higher intensity of the H_{alpha} peak it was monitored as a function of the RF power, and is shown in Figure 2D. As the RF power increases, the intensity of the H_{alpha} peak increases until around 100 W, where it

asymptotes. This indicates that we have maximum hydrogen cracking of the propylene at 100 W. Increased cracking of hydrogen in the propylene molecule is highly desirable for developing higher density diamond-like carbon films desired for ICF ablator application. A future obstacle to overcome is that the optimal power for hydrogen cracking occurs above the threshold bias voltage for etching, making the development of denser films more difficult. A potential solution would be to use a lighter diluting gas (such as neon) that will not sputter as rapidly during deposition.

Film stresses calculated from the radius of curvature of the coated substrates is shown in Table 2. To date, there is no clear correlation between the plasma conditions and the film stress. The stresses for films overall (67-113 MPa) are much lower overall compared to diamond like carbon films produced by other methods such as cathodic arc which have stresses in the GPa range [12, 14-15]. One of the major successes of this project was that a 45 μm-thick film with significantly low stress (67 MPa) was able to be deposited.

Table 2. Film Stresses at Different RF powers and Thicknesses.

Film Thicknesses and Stresses		
Power (W)	Thickness (um)	Stress (MPa)
25 W	1.58 um	88±4
60 W	45.43 um	67±1
75 W	3.98 um	113±6

Atomic force microscopy (AFM) on the 45 μm-thick DLC film, measured a very fine grain structure with amorphous grain sizes in the order of 20 nm and a root-mean-square surface roughness of 0.5 nm. This is close to roughness of the initial silicon substrate. The combination of very low surface roughness and an ultra-fine grain size distribution in the nanometer scale makes these films promising for ICF applications.

Raman spectroscopy was taken on a series of samples grown with N2 as the diluting gas as a function of RF power. The shape of the spectrum indicated that these samples are amorphous, which was also verified via X-Ray diffraction measurements which also displayed no graphite diffraction peaks. Further analysis of the structure is planned.

RBS and ERDA measurements were used to extract the elemental film composition and density. A representative RBS spectrum is shown in Fig. 3, revealing the presence of C, N, O, and Fe through the thickness of the sample. H-content was calculated utilizing ERDA. Iron contamination is consistent through the trials (4 at%) and most likely comes from sputtering of the stainless-steel hollow cathode. The atomic composition from RBS and hydrogen content from ERDA are shown in Table 3. The diluting gas N_2 is also incorporated into the samples at a constant 11 at% except for the film grown at 25 W, likely

due to lower nitrogen ionization at lower powers. The ERDA indicates the power does not have a significant effect on the H-content until higher power thresholds are reached (<50W).

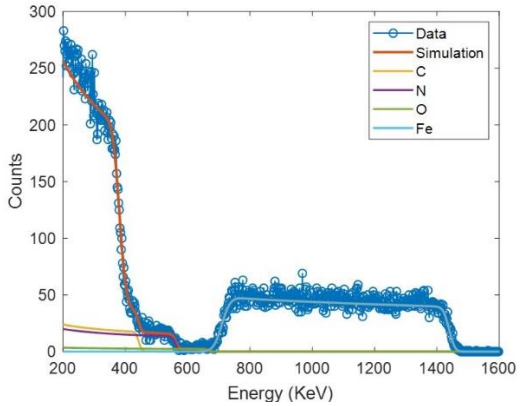

Figure 3. RBS spectrum of a 1.6 µm-thick a-C:H film.

RF Power (W)	25	50	60	75	85
C (at. %)	62.1	51.2	52.3	55.5	59.7
H (at. %)	29	31	28	26	21
N (at. %)	3.6	13.1	11.2	11.2	11.8
O (at. %)	1.1	1.3	5.7	2.9	3.6
Fe (at. %)	4.2	3.4	2.8	4.4	3.9

Table 3. Atomic composition of a-C:H films as a function of RF power.

RBS measurements were used to calculate the film density and were compared to those measured by the weight of the coating. Depending on the measurement type, the density varies between 1.1-1.2 and 1.6-1.7 g/cc as the RF-power is increased from 25 to 75 W. Between 25W and 75W the films deposited change from transparent (as seen by interference fringing) to a shiny black coating, indicating a structural change in the applied coating.

This corresponds with the increase in sp3 content measured via Raman spectroscopy, which would also indicate higher density films.

Impact on Mission

Hard, dense, amorphous carbon films are desirable for laser-fusion target ablators, and other applications. Although not the emphasis of this project, they would also be desirable for environmental protection of fiber optics, and coatings on medical implants. This project also provided an opportunity for new staff members to gain experience in coating and vacuum technology. The capabilities of the hollow-cathode plasma source were also explored, extending its range of use beyond its previous use as a low-energy oxygen plasma source for etching diamond anvils

Conclusion

In this project, we have developed low stress, amorphous hydrogenated carbon films up to 45 µm-thick with density up to 1.7 g/cc. This exceeds the density of GDP ablators and is approaching the density of beryllium. There is still a significant amount of work required to close the gap between current film densities and high-density diamond-like carbon.

Atomic force microscopy (AFM) on the 45 µm-thick DLC film, measured a very fine grain structure with amorphous grain sizes in the order of 20 nm and a root-mean-square surface roughness of 0.5 nm. This is close to roughness of the initial silicon substrate. The combination of very low surface roughness and an ultra-fine grain size distribution in the nanometer scale makes these films promising for ICF applications.

This work will continue in our FY20 LDRD project. The addition of dopants to the films will be explored as well.

References

[1] Kritcher, A.L.; Clark, D.; Haan, S.; Yi, S.A.; Zylstra, A.B.; Callahan, D.A.; Hinkel, D.E. Berzak Hopkins L.F.; hurricane, O.A; Landen, O.L.; Maclaren, S.A; Meezan, N.B.; Patel, P.K.; Ralph, J; C.A. Thomas, Town, R.; Edwards, M.J. Comparison of plastic, high density carbon, and beryllium as indirect drive NIF ablators. Physics of Plasma, 2018, 25, 056309, https://doi.org/10.1063/1.5018000

[2] Clark, D.S.; Kritcher, A.L; Yi, S.A.; Zylstra, A.B.; Haan, S.W. and C.R. Weber. Capsule physics comparison of National Ignition facility implosion designs using plastic high density carbon, and beryllium ablators. 2018, 25, 032703. https://doi.org/10.1063/1.5016874

[3] Clark, D,; Haan, S; Hammel, B.; Salmonson, J.; Callahn, D. and R. Town. Plastic ablator ignition capsule design for the National Ignition Facility. Physics of Plasmas, 2010 17, 052703. doi:10.1063/1.3403293

[4] Ali, S.J.; Celliers, P.M., Haan, S.W.; Boehly, T.R.; Whiting, N.; Baxamusa, S.H.; Reynolds, H.; Johnson, M.A.; Hughes, J.D.; Watson, B.; Engelhorn, K.; Smalyuk, V.A; and Landen, O.L. Hydrodynamic instability seeding by oxygen nonuniformities in glow discharge polymer inertial fusion ablators. Physical Review E, 2018, 98, 033204. DOI: 10.1103/PhysRevE.98.033204

[5] Wilson, D.; Bradley, P.; Hoffman, N.; Swenson, F. Smitherman, D.;Chrien, R.; Margevicius, Thoma, D.J.; Foreman, L.; Hoffer, J.; Robert Goldman, S., Caldwell, S.; Dittrich, T.; Haan, S.; Marinak, M.; Pollaine, S.; and J. Sanchez. Physics of Plasmas, 1998, 5, 1953. https://doi.org/10.1063/1.872865

[6] Biener, J.; Mirkarimi, P.; Tringe, J.; Baker, S.; Wang, Y.; Kucheyev, S.; Teslich, N.; Wu, K.; Hamza, A.; Wild, C.; Woerner, E.; Koidl, P.; Bruehne, K.; and Fecht, J. Diamond Ablators for Inertial Confinement Fusion. *Fusion Science and Technology, 2017,* 49:4, 737-742. https://doi.org/10.13182/FST49-737

[7] Pereira Fenili, C.; Silvio de Souza, F.; Marin, G.; Maria Hickel Probst, S.; Binder, C.; Nelmo Klein, A. Corrosion resistance of low-carbon steel modified by plasma nitriding

and diamond-like carbon. Diamond and related Materials, 2017, 80, 153-161. https://doi.org/10.1016/j.diamond.2017.11.001
[8] Ankit, K.; Varade, A.; Reddy, N.; Dhan, S.; M., Chellamalai.; Balashanmugam, N; Krishna, P. Synthesis of high hardness IR optical Coatings using diamond-like carbon by PECVD at room temperature. 2017, 78, 39-43. http://dx.doi.org/10.1016/j.diamond.2017.07.008
[9] Tsai, P.; Huang, H.; Sung, C.; Kan, M.; and Y. Wang. High-Power LED Chip-on-Board Packages With Diamond-Like Carbon Heat-Spreading Layers. Journal of Display Tehcnology, 2016, 12, 357-361. 10.1109/JDT.2015.2491934
[10] Ghosh, B.; Guzman-Olivos.; and R. Espinoza-Gonzalez. Plasmon-enhanced optical absorption with graded bandgap in diamond-like carbon films. J Mater Sci, 2017, 52, 218-228. DOI 10.1007/s10853-016-0324-7
[11] Grill, A. Diamond-Like carbon: state of the art. *Diamond and Related Materials, 8* 1999, 428-434.
[12] Falabella, S.; Boercker, D.B.; and D.M., Sanders. Fabrication of amorphous diamond films. Thin solid films, 1993, 236, 82-86.
[13] Sheeja, D.; Tay, B.K.; Leong, K.W.; and Lee, C.H. Effect of film thickness on the stress and adhesion of diamond-like carbon coatings. Diamond and related Materials, 2002, 11, 1643-1647.
[14] Wang, P.; Wang, X.; Xu, T.; Liu, W.; and j, Zhang. Comparing internal stress in diamond-like carbon films with different structure. 2007, 515, 6899-6903.
[15] Lossy, R. Pappas, D.; Ronnen, R.; Doyle, J.; and J. Cuomo. Properties of amorphous diamond films prepared by a filtered cathodic arc. Journal of Applied Physics, 1995, 77, 4750. https://doi.org/10.1063/1.359411
[16] Tsai, P.; K. Chen. Evaluation of microstructures and mechanical properties of diamond like carbon films deposited by filtered cathodic arc. Thin Solid Films 516 (2008) 5440—5444.
[17] ultrathin diamond like carbon films deposited by filtered carbon vacuum arcs. IEEE transactions on plasma science, Vol. 29, No. 5, October 2001.
[18] Synthesis of hydrogenated diamondlike carbon thin films using neon-acetylene based high power impulse magnetron sputtering discharges. Journal of vacuum Science and Technology. 34, 061504 (2016). doi: 10.1116/1.4964749
[19] Thick diamond like carbon coatings deposited by deep oscillation magnetron sputtering. Surface & Coatings Technology 315 (2017) 294–302. http://dx.doi.org/10.1016/j.surfcoat.2017.02.044
[20] Optical, structural, and bonding properties of diamond-like amorphous carbon films deposited by DC magnetron sputtering. Diamond & Related Materials 56 (2015) 29–35. https://doi.org/10.1016/j.diamond.2015.04.004
[21] Correlations between microstructure and hydrophobicity properties of pulsed laser deposited diamond-like carbon films. Superlattices and Microstructures 81 (2015) 64–79. http://dx.doi.org/10.1016/j.spmi.2014.11.041
[22] Diamond-like carbon film with gradient germanium-doped buffer layer by pulsed laser deposition. Surface & Coatings Technology 337 (2018) 290–295. https://doi.org/10.1016/j.surfcoat.2018.01.023

[23] Tribological behavior of diamond-like carbon thin films deposited by the pulse laser technique at different substrate temperatures. Tribology International 103 (2016) 274–280. http://dx.doi.org/10.1016/j.triboint.2016.07.013.
[24] Diamond-like carbon thin film deposition using a magnetically r.f. PECVD system. Diamond and Related Materials 4 (1995) 977-983
[25] Properties and structures of diamond-like carbon film deposited using He, Ne, Ar/ methane mixture by plasma enhanced chemical vapor deposition. Journal of Applied Physics 87, 8122 (2000); https://doi.org/10.1063/1.373507

[26] Fast deposition of diamond-like carbon films by radio frequency hollow cathode method. Thin Solid Films 534 (2013) 226–230. http://dx.doi.org/10.1016/j.tsf.2013.02.123

[27] Investigation of diamond-like carbon films synthesized by multi-jet hollow cathode rf plasma source. Thin Solid Films 406 (2002) 275–281.

[28] Mechanical properties of DLC films prepared in acetylene and methane plasmas using electron cyclotron resonance microwave plasma chemical vapor deposition. Diamond and Related Materials 10 Ž2001. 1862_1867.

[29] Photo-oxidation of polymer-like amorphous hydrogenated carbon under visible light illumination. Polymer Degradation and Stability 122 (2015) 133e138. http://dx.doi.org/10.1016/j.polymdegradstab.2015.11.001

[30] Ultralow Stress, Thermally Stable Cross-Linked Polymer Films of Polydivinylbenzene (PDVB). Langmuir 2017, 33, 5204−5212. DOI: 10.1021/acs.langmuir.7b01403

[31] Improved planar radio frequency inductively coupled plasma configuration in plasma
immersion ion implantation. Review of Scientific Instruments 74, 2704 (2003); https://doi.org/10.1063/1.1568559

[32] Electron Cyclotron Resonance in a Weakly Magnetized Radio-Frequency Inductive Discharge. Physical Review Letters, 2002, 88 (9). 10.1103/PhysRevLett.88.095002

[33] Some effects of magnetic field on a hollow cathode ion source. Review of Scientific Instruments, 2004, 75 (4), DOI: 10.1063/1.1651633

[34] SIMNRA, a simulation program for the analysis of NRA, RBS and ERDA. AIP Conference Proceedings 475, 541 (1999). M. Mayer. https://doi.org/10.1063/1.59188
[35] Interpretation of Raman spectra of disordered and amorphous carbon. A. C. Ferrari and J. Robertson. Physical Review B, 61(20):13, 2000.
[36] Resonant raman spectroscopy of disordered, amorphous, and diamondlike carbon. A. C. Ferrari and J. Robertson. Physical Review B, 64(7), 2001.

[37] Raman spectroscopy of amorphous, nanostructured, diamond-like carbon, and nanodiamond. A. C. Ferrari and J. Robertson. Philosophical Transactions of the Royal Society of London A, 362:36, 2004.
[38] Subplantation model for film growth from hyperthermal species. Y. Lifshitz, S. R. Kasi, J. W. Rabalais, and W. Eckstein. Physical Review B, 41(15):10468{10480, 1990.

Publications and Presentations

A publication describing the results to date is in preparation.

Notes to the Editors

The H_{alpha} and the H_{beta} symbols can be replaces by the Greek letters "alpha" and "beta"

"45 µm" is the abbreviation for micrometers.